Semiconductor Physics, Quantum Electronics & Optoelectronics, 2024. V. 27, No 1. P. 109-116.

Optoelectronics and optoelectronic devices

Numerical study of single-layer and interlayer grating polarizers based on metasurface structures for quantum key distribution systems

A.Q. Baki, S.K. Tawfeeq*

Institute of Laser for Postgraduate Studies, University of Baghdad, Al-Jadyriah, 10070, Baghdad, Iraq
**Corresponding author e-mail: shelan.khasro@ilps.uobaghdad.edu.iq*

Abstract. Polarization is an important property of light, which refers to the direction of electric field oscillations. Polarization modulation plays an essential role for polarization encoding quantum key distribution (QKD). Polarization is used to encode photons in the QKD systems. In this work, visible-range polarizers with optimal dimensions based on resonance grating waveguides have been numerically designed and investigated using the COMSOL Multiphysics Software. Two structures have been designed, namely a single-layer metasurface grating (SLMG) polarizer and an interlayer metasurface grating (ILMG) polarizer. Both structures have demonstrated high extinction ratios, $\sim 1.8 \cdot 10^3$ and $8.68 \cdot 10^4$, and the bandwidths equal to 45 and 55 nm for the SLMG and ILMG, respectively.

Keywords: quantum cryptography, resonance grating, subwavelength grating, metasurfaces, wire grid polarizer.

https://doi.org/10.15407/spqeo27.01.109
PACS 03.67.Dd, 42.79.Dj, 42.82.Et

Manuscript received 17.10.23; revised version received 08.01.24; accepted for publication 28.02.24; published online 12.03.24.

1. Introduction

Unpolarized light with randomly oriented oscillations is converted into linearly, circularly, or elliptically polarized light waves using polarizers and wave plates. When light travels a distance substantially greater than its wavelength, conventional optical components that control the polarization state are often based on the accumulated phase shift between two orthogonally polarized electric fields. Therefore, conventional polarization optics is bulky and limits the possibility of miniaturization and dense integration in advanced photonic devices and systems [1].

Modern trends imply miniaturizing and searching for alternative methods to control light at extremely small dimensions. Accordingly, compact devices with new functionalities need to be realized using artificial optical materials [2].

Metamaterials are three-dimensional (3D) artificial composite nanostructures with innovative optical properties that enable guiding and controlling electromagnetic waves to obtain novel optical effects not achievable with natural materials, and offer new applications. The latter are still challenging because of the difficulty of fabricating complex 3D structures. Moreover, intrinsic metallic losses of plasmonic elements at optical frequencies limit the efficiency of such structures [3]. To overcome these difficulties, metasurfaces, which are the two-dimensional (2D) equivalents of metamaterials, have emerged as a new model for designing optical elements [4]. Furthermore, dielectric metasurfaces with extremely low losses have been proposed to further enhance efficiency [5].

In quantum key distribution (QKD) systems, two remote parties, traditionally called Alice and Bob, are allowed to exchange unconditionally secure keys. Subsequent check of their secrecy is based on the quantum mechanic principles [6]. QKD is considered as one of the first practical applications based on single photons [7].

All-dielectric metasurfaces with novel polarization control capabilities can be efficiently applied in QKD systems and other quantum optics applications for data encryption and detection [4].

For example, according to the BB84 protocol, photons emitted from single-photon sources require polarizers and half-wave plates to prepare photons randomly polarized at 0°, 45°/−45° and 90° at the Alice's side. These polarized photons are sent to Bob through the quantum channel. The received photons are randomly analyzed along one of the four directions. If the same polarization basis, *i.e.*, rectilinear (0° and 90°) or diagonal (45° and −45°) is used by Bob then perfect correlation between Alice and Bob is achieved [8].

Basically, QKD implements one-way protocols such as *e.g.* the BB84 protocol, according to which qubits are prepared and then sent by Alice to Bob. The incoming qubits are measured by Bob to decode the raw key bits.

Alternative approaches to QKD and quantum communication research in general employ two-way protocols, according to which qubits are prepared by Bob and then sent to Alice. Alice encodes classical information onto the quantum states of the incoming qubits and then sends them back to Bob. Finally, measurements are performed by Bob to decode the messages [9].

Many protocols such as BB84, E91, BBM92, B92, SSP, DSP, SARG04, COW [10] and MDI-QKD [11] are presently available for implementing QKD systems.

New technologically feasible and highly secure approaches are also proposed. They are based on the concept of involving hybrid algorithms such as the BB84 protocol and genetic algorithm in cloud security [12], or using the BB84 protocol with the Advanced Encryption Standard (AES) algorithm in wireless sensor networks [13].

Metasurfaces enable light manipulation using a 2D array of optical scatterers separated by subwavelength spacings. The metasurfaces are formed by structured metallic or dielectric nanoparticles or subwavelength apertures in metallic or dielectric thin films. The amplitude and phase of the incoming light can be modulated by metasurfaces with the thickness much smaller than the light wavelength [2].

Another essential property of all-dielectric metamaterials is the possibility to engineer the anisotropy of the media where high refractive index contrast can be achieved. Increase of this contrast enables a control of the light polarization by all-dielectric metasurfaces far beyond the capabilities of traditional diffractive or refractive optical elements having the principal refractive indices for the two possible polarizations (extraordinary and ordinary) rarely exceeding 10% [14].

Dielectric materials such as Si, TiO_2, SiO_2 and Si_3N_4 emit light with the wavelengths in the visible and near IR spectral region. They have very low optical losses and are mechanically and chemically robust [2]. These materials are considered as platforms for highly efficient metasurfaces. Among them, Si is widely available and can be easily processed using the standard CMOS-compatible techniques. Therefore, Si-based metasurfaces are considered as low-cost metasurface platforms. At this, however, Si is not optically transparent, which limits its applications in the visible range. Therefore, development of high-efficiency metasurfaces focuses on the TiO_2-based metasurfaces, which have a high refractive index, low optical losses and exhibit exceptional properties in the visible range [5].

In the previous works, wire grid polarizers (WGP) made from different dielectric materials and operating at different wavelengths were designed. The important WGP characteristics include the extinction ratio (ER) and the operation band. Earlier, a broadband polarizer having the operation range of 0.3 to 5 μm, the transmission efficiency over 60% and the average extinction ratio above 70 dB was proposed [15]. A single-layer high-index contrast polarizer with the 95% reflection and transmission efficiencies for both TE and TM polarization was designed by Zheng *et al*. [16]. The ER of transmission of this polarizer was higher than 30 dB. Using Si nanowire arrays, Yoon *et al*. achieved a 200-nm-wide band of high reflection for one polarization state and free transmission for the orthogonal state [17]. A TiO_2 WGP was designed and fabricated by Siefke *et al*. This WGP had the ER of 384 and transmittance of 10% at the wavelength of 193 nm [18]. Ranjbar *et al*. investigated cascaded all-dielectric metasurfaces that consisted of stacked high-contrast subwavelength gratings with varied crystal axes. With such metasurfaces, multiband and multifunctional polarization control in the IR region was realized [19]. Hemmati *et al*. designed a stack of two dual-grating modules with the ER of ∼100,000 across a 50 nm bandwidth in the telecommunications spectral region [20]. This work was followed by fabrication of a compact high-efficiency resonant polarizer using a Si-on-SiO_2 material system. The efficiency of such polarizer was improved by creating a cascaded dual-module system consisting of fundamental subwavelength grating building elements. The ER value of ∼3000 across a bandwidth of ∼110 nm in the spectral range of 570 to 680 nm was obtained [21].

In this paper, we design and investigate the performance of single-layer and interlayer metasurface grating polarizers in the visible spectral region. The structures were composed of TiO_2 thin films on a SiO_2 substrate. The operation of both polarizers is based on the guided mode resonance effect.

This paper is organized as follows. Section 2 describes the single-layer and interlayer metasurface grating structures. The performance of both polarizers is evaluated by finding their extinction ratio values. Section 3 presents the study of the fabrication tolerance of both polarizers. Finally, Section 4 provides the conclusions of the work.

2. Design of single-layer and interlayer metasurface grating polarizers

A resonance grating waveguide (RGW) structure has a multilayer configuration comprising a substrate and a thin dielectric or semiconductor waveguide layer. The grating is etched on an additional layer. Operation of this structure is based on the guided-mode resonance effect [22]. When an incident light beam strikes an RGW structure, some of the light is transmitted directly, while the rest is diffracted and trapped in the waveguide layer. Then the trapped light is partially diffracted outwards and destructively interferes with the transmitted part of the light beam. The RGW structure “resonates” (total interference takes place and no light is transmitted) at a particular wavelength and angular orientation of the incident beam. The waveguide layer thickness, the grating depth and the grating fill factor all have an impact on the resonance bandwidth [22].

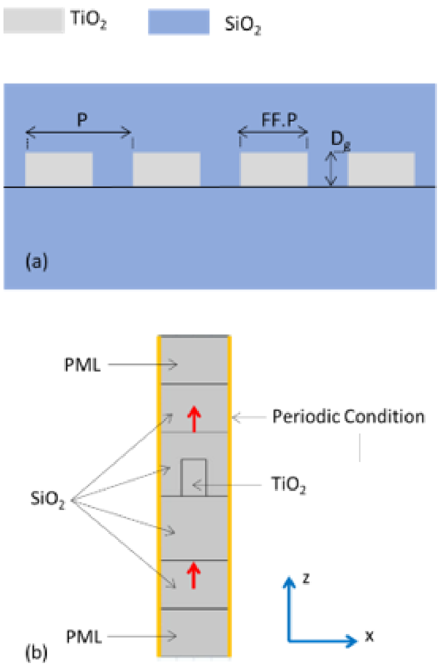

Fig. 1. Single-layer metasurface grating structure (a). Simulation model (b).

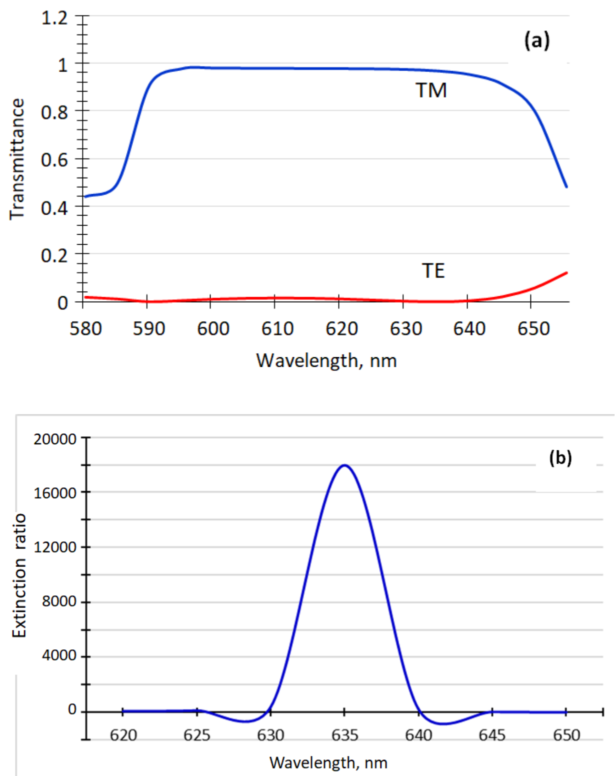

Fig. 2. Single-layer metasurface grating polarizer. Transmittance of TM and TE polarized states (a). ER of single-layer metasurface grating polarizer, where P, D_g and FF are equal to 400, 231 and 0.355 nm, respectively (b).

Fig. 1 schematically shows the structure of the designed polarizer containing a single-layer metasurface grating (SLMG). Based on the guided-mode resonance effect, the designed structure transmits the TM polarization state and blocks the TE state. The structure consists of a TiO_2 film on a 700 nm thick SiO_2 substrate. The grating is covered by a 1000 nm thick SiO_2 layer. The refractive indices of TiO_2 and SiO_2 are 2.5824 and 1.4570 at $\lambda = 635$ nm, respectively. The optimum values of the geometrical parameters of the SLMG grating, *i.e.*, the grating period (P), grating thickness (D_g), and fill factor (FF), were found in a 2-D framework using the Monte Carlo optimization method implemented in the COMSOL Multiphysics Software environment. In this method, the geometrical parameters of the grating are randomly sampled with equal probabilities within a user-specified limit. This limit includes the values of the grating geometrical parameters within the accepted range. Table 1 lists the limits for optimization of the SLMG geometrical parameters.

Table 1. Limits for SLMG geometrical parameters optimization.

Geometrical parameter	Lower limit	Upper limit	Resolution
D_g	100 nm	400 nm	10 nm
P	200 nm	600 nm	10 nm
FF	0.1	0.9	0.1

The Monte Carlo solver is efficient for collecting statistical data related to variations of the design parameters by analyzing the range of value of the objective function that is maximized (or minimized) considering several constraints.

The optimum dimensions ensure maximum transmittance for the TM polarization and minimum transmittance for the TE polarization states. The optimum values of P, D_q and FF are 400, 231 and 0.355 nm, respectively. Fig. 2a shows the transmittance of light for the zero-order TM polarization. The extinction ratio, defined as ER = T_{TM}/T_{TE}, *versus* light wavelength is shown in Fig. 2b. As can be seen from this figure, the maximum ER value is ~$1.8\cdot10^3$ at $\lambda = 632$ nm.

The maps of the TM and TE state transmission as functions of FF for the SLMG are shown in Figs 3a and 3b, respectively. The effect of P on the TM and TE transmission is shown in Figs 3c and 3d, respectively. The high and low transmissions are indicated by the dark red and dark blue areas, respectively. The white dashed lines show the FF and P values corresponding to the maximum transmission of the TM polarization state.

Since TiO_2 has no losses in the visible spectral region, two SLMGs can be interlayered as shown in Fig. 4. The resulting new polarizer, which consists of two interlayer metasurface gratings (ILMG), would improve the polarizer performance.

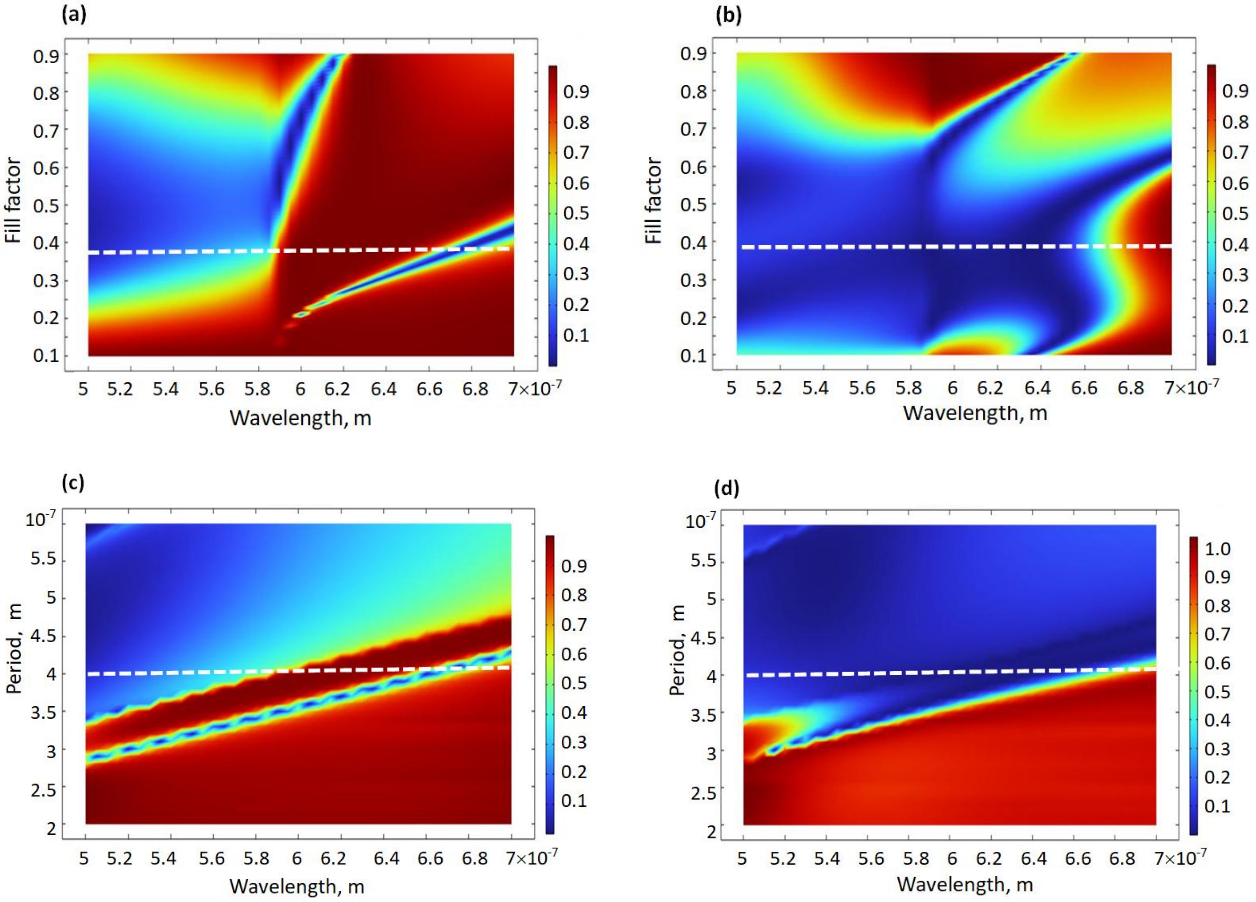

Fig. 3. Transmission map of the single-layer metasurface grating polarizer as a function of fill factor for TM (a) and TE (b) polarization states, period for TM (c) and TM (d) polarization states. (Color online)

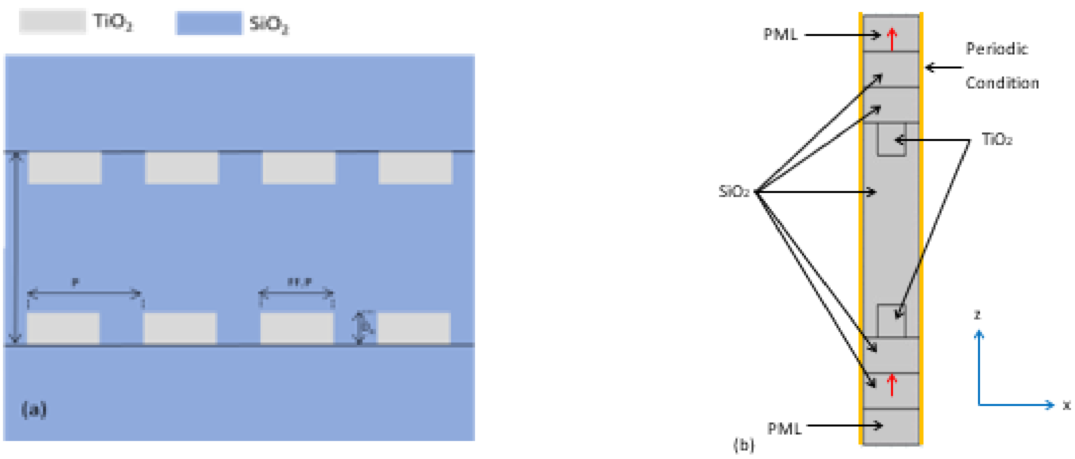

Fig. 4. Interlayer metasurface grating structure (a). Simulation model (b).

The thickness of the gap between the two layers is very important to avoid the unwanted Fabry–Perot resonance between the upper and lower gratings. The upper and the lower SLMGs are both high reflectors for the TE polarization state and will form a Fabry–Perot cavity. In our ILMG structure, SiO_2 with the thickness D_{gap} = 1200 nm was chosen as a gap material.

The optimum ILMG dimensions to maximize transmittance for the TM polarization state and suppress it for the TE polarization state were found in the 2-D framework using the Monte Carlo optimization method. Table 2 lists the limits for the ILMG geometrical parameters optimization.

The optimum values of P, D_g and FF are equal to 373, 180 and 0.451 nm, respectively. Fig. 5a shows the transmittance of the TM and TE polarization states and Fig. 5b shows the ER value, which is approximately equal to $8.68 \cdot 10^4$ at λ = 590 nm.

Table 2. Limits for ILMG geometrical parameters optimization.

Geometrical parameter	Lower limit (nm)	Upper limit (nm)	Resolution
D_g	100 nm	300 nm	10 nm
P	200 nm	500 nm	10 nm
FF	0.1	0.9	0.1

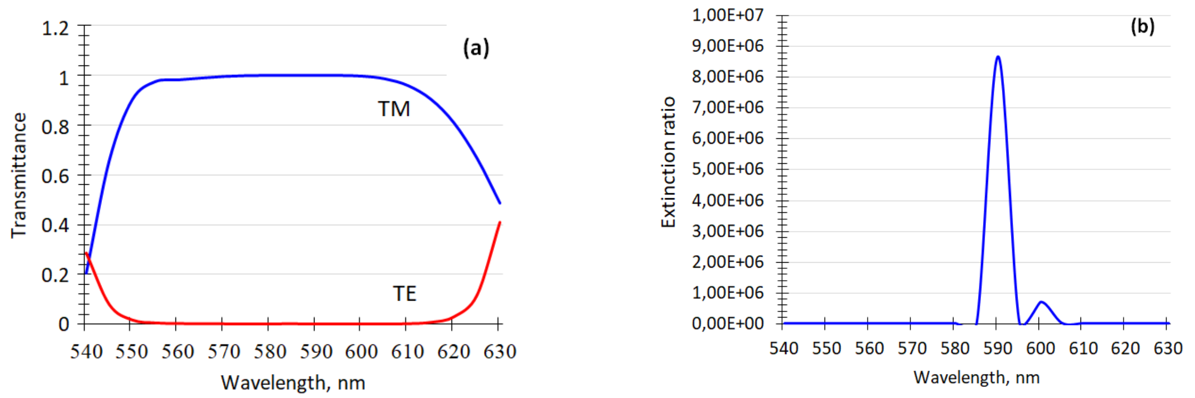

Fig. 5. Interlayer metasurface grating polarizer. Transmittance of the TM and TE polarized states (a). ER of the interlayer metasurface grating polarizer, where P, D_g and FF are equal to 373, 180 and 0.451 nm, respectively (b).

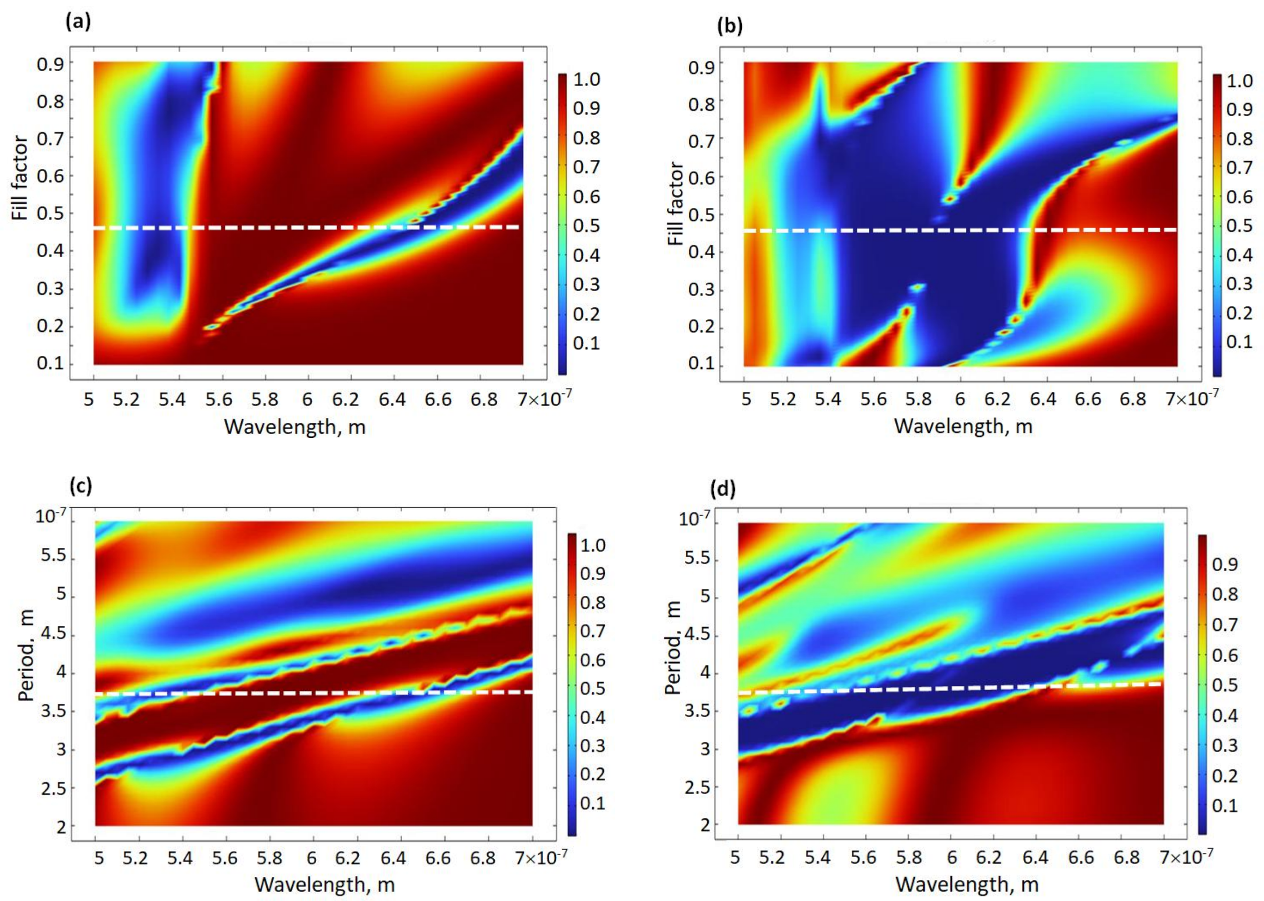

Fig. 6. Transmission of the interlayer metasurface grating polarizer as a function of fill factor for the TM (a) and TE (b) polarization states as well as period for the TE (c) and TM (d) polarization states. (Color online)

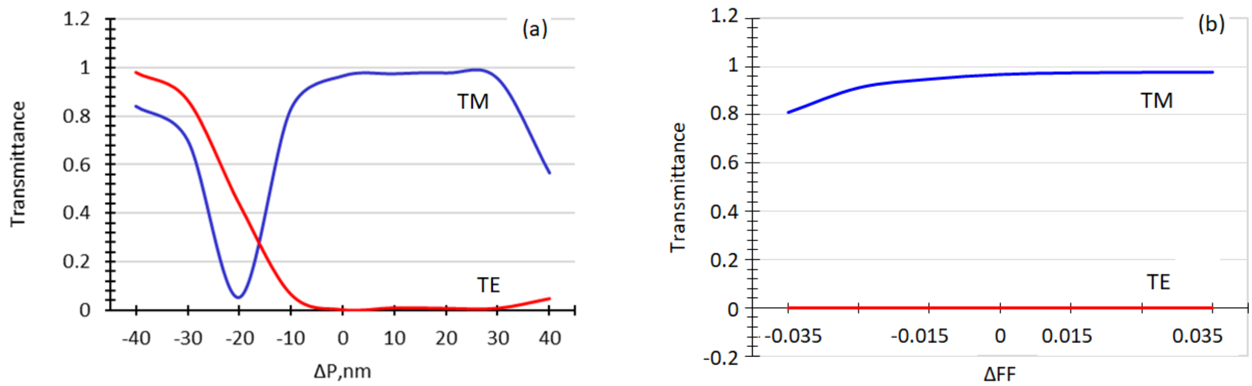

Fig. 7. Fabrication tolerance of the single-layer metasurface grating polarizer to *P* (a) and FF (b).

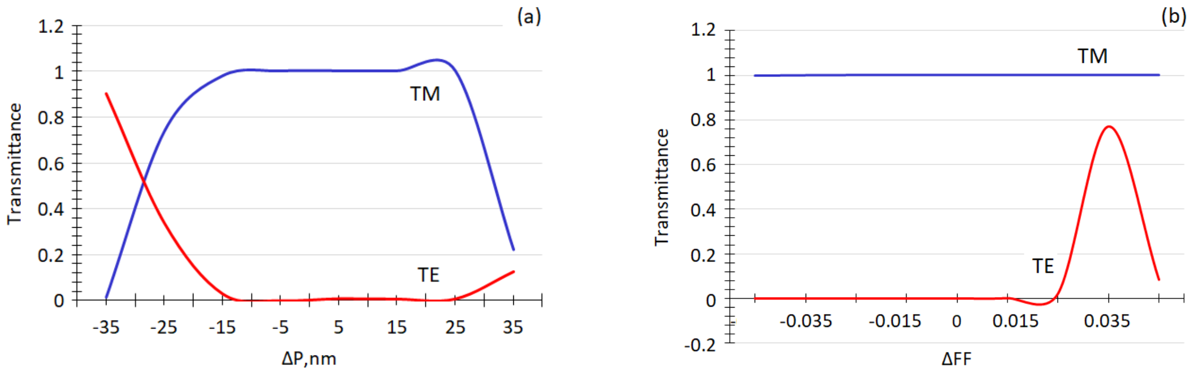

Fig. 8. Fabrication tolerance of the interlayer metasurface grating polarizer to *P* (a) and FF (b).

Fig. 6 shows the transmission maps for the TM and TE states of the ILMG polarizer as functions of FF and *P*. The designed SLMG and ILMG structures can be used as polarizers for transmitting the TE and ± 45° polarization states by rotating the SMLG or ILMG structures by 90° and ± 45°. These polarization states are used to encode photons in QKD systems.

3. Fabrication tolerance

Atomic layer deposition method was used for fabricating metasurface gratings [23]. Since the optimum grating dimensions cannot be precisely obtained in the deposition process, the fabrication tolerance to the grating width was studied for both the SLMG and ILMG polarizers by measuring transmittance at the non-optimal values of *P* and FF. Fig. 7 shows the fabrication tolerance for the SLMG polarizer. Zero Δ*P* and ΔFF correspond to the optimum values of *P* and FF. It can be seen from Fig. 7 that the tolerance to *P* is more critical than to FF. The tolerance to *P* ranges within 400…430 nm, while that to FF is in the range of 0.3495…0.3895.

The ILMG polarizer fabrication tolerance is shown in Fig. 8. As can be seen from this figure, the tolerance to *P* ranges within 366…386 nm. FF shows an excellent tolerance in the range of 0.4059…0.4659. These results allow one to conclude that the tolerance range of the grating period is ≅ +23 nm for the SLMG and ≅ µ10 nm for the ILMG polarizer.

4. Conclusion

Using the COMSOL Multiphysics Software, an optical polarizer based on resonance grating waveguide was numerically designed and investigated. TiO_2 was used as a grating material. The polarizer dimensions were optimized by the Monte Carlo optimization method implemented in the COMSOL Multiphysics Software environment. The accepted ER values ~$1.8 \cdot 10^3$ and ~$8.68 \cdot 10^4$ in the visible spectral region were obtained for the SLMG and ILMG polarizers, respectively. The metasurface-based polarizers studied in this work are compact and compatible with transmitters in QKD systems. Although the ILMG structure is more complicated than the SLMG one, the deviation of the SLMG grating width (16 nm) is more critical than that of the ILMG grating (23 nm).

Acknowledgment

The authors are grateful to Dr. Farooq A. Khaleel for his support and valuable comments.

References

1. Intaravanne Y., Chen X. Recent advances in optical metasurfaces for polarization detection and engineered polarization profiles. *Nanophotonics*. 2020. **9**, No 5. P. 1003–1014. https://doi.org/10.1515/nanoph-2019-0479.
2. Choudhury S.M., Wang D., Chaudhuri K. *et al*. Material platforms for optical metasurfaces.

Nanophotonics. 2018. **7**, No 6. P. 959–987. https://doi.org/10.1515/nanoph-2017-0130.
3. Hsiao H., Chu C.H., Tsai D.P. Fundamentals and applications of metasurfaces. *Small Methods*. 2017. **1**, No 4. https://doi.org/10.1002/smtd.201600064.
4. Yueqiang H., Xudong W., Xuhao L. *et al.* All-dielectric metasurfaces for polarization manipulation: Principles and emerging applications. *Nanophotonics*. 2020. **9**, No 12. P. 3755–3780. https://doi.org/10.1515/nanoph-2020-0220.
5. Hsu W., Chen Y., Yeh S. *et al*. Review of metasurfaces and metadevices: Advantages of different materials and fabrications. *Nanomaterials*. 2022. **12**, No 12. P. 1973. https://doi.org/10.3390/nano12121973.
6. Mushatet A.F., Tawfeeq S.K. Modeling and simulation for performance evaluation of optical quantum channels in quantum key distribution systems. *Al-Khwarizmi Eng. J.* 2021. **17**, No 2. P. 31–44. https://doi.org/10.22153/kej.2021.05.001.
7. Salih S.M., Tawfeeq S.K., Khaleel A.I. Generation of true random TTL signals for quantum key distribution systems based on true random binary sequences. *Iraqi J. Laser*. 2019. **18**, No 1. P. 31–42. https://doi.org/10.31900/ijl.v18i1.188.
8. Salih S.M., Tawfeeq S.K. Random signal generation and synchronization in lab-scale measurement device-independent – quantum key distribution systems. *J. Opt. Technol*. 2019. **86**, No 3. P. 137–143. https://doi.org/10.1364/JOT.86.000137.
9. Chen H., Zhou Z., Zangana A. *et al*. Experimental demonstration on the deterministic quantum key distribution based on entangled photon. *Sci. Rep*. 2016. **6**. P. 20962. https://doi.org/10.1038/srep20962.
10. Nurhadi A.I., Syambas N.R. Quantum Key Distribution (QKD) Protocols: A Survey. *2018 4th Int. Conf. on Wireless and Telematics (ICWT)*, 2018. https://doi.org/10.1109/ICWT.2018.8527822.
11. Khaleel A.I., Tawfeeq S.K. Key rate estimation of measurement-device-independent quantum key distribution protocol in satellite-earth and inter-satellite links. *Int. J. Quantum Inf*. 2018. **16**, No 3. https://doi.org/10.1142/S0219749918500272.
12. Kumar J., Saxena V. Cloud data security through BB84 protocol and genetic algorithm. *Baghdad Sci. J*. 2022. **19**, No 6. P. 1445–1453. https://dx.doi.org/10.21123/bsj.2022.7281.
13. Alhasnawy L.H., AL-Mashanji A.K. Improving wireless sensor network security using quantum key distribution. *Baghdad Sci. J*. 2023. **20**, No 5 (Suppl.). https://doi.org/10.21123/bsj.2023.7460.
14. Jahani S., Jacob Z. All-dielectric metamaterials. *Nat. Nanotechnol*. 2016. **11**. P. 23–36. https://doi.org/10.1038/nnano.2015.304.
15. Yang Z.Y., Lu Y.F. Broadband nanowire-grid polarizers in ultraviolet-visible-near-infrared regions *Opt. Express*. 2007. **15**, No 5. P. 9510–9519. https://doi.org/10.1364/OE.15.009510.
16. Zheng G., Cong J., Xu L. *et al*. Compact polarizers with single layer high-index contrast gratings. *Infrared Phys. Technol*. 2014. **67**. P. 408–412. https://doi.org/10.1016/j.infrared.2014.09.012.
17. Yoon J.W., Lee K.J., Magnusson R. Ultra-sparse dielectric nanowire grids as wideband reflectors and polarizers. *Opt. Express*. 2015. **23**, No 22. P. 28849–28856. https://doi.org/10.1364/OE.23.028849.
18. Siefke T., Kroker S., Pfeiffer K. *et al.* Materials pushing the application limits of wire grid polarizers further into the deep ultraviolet spectral range. *Adv. Opt. Mater*. 2016. **4**, No 11. P. 1780–1786. https://doi.org/10.1002/adom.201600250.
19. Ranjbar A., Grbic A. Broadband, multiband, and multifunctional all-dielectric metasurfaces. *Phys. Rev. Appl*. 2019. **11**, No 5.
20. Hemmati H., Bootpakdeetam P., Magnusson R. Metamaterial polarizer providing principally unlimited extinction. *Opt. Lett*. 2019. **44**, No 22. P. 5630–5633. https://doi.org/10.1364/OL.44.005630.
21. Bootpakdeetam P., Hemmati H., Magnusson R. Cascaded metamaterial polarizers for the visible region. *Opt. Lett*. 2020. **45**, No 24. P. 6831–6834. https://doi.org/10.1364/OL.411234.
22. Rosenblatt D., Sharon A., Friesem A. Resonant grating waveguide structures. *IEEE J. Quantum Electron*. 1997. **33**, No 11. P. 2038–2059. https://doi.org/10.1109/3.641320.
23. Ikeda K., Takeuchi K., Takayose K. *et al*. Polarization-independent high-index contrast grating and its fabrication tolerances. *Appl. Opt*. 2013. **52**, No 5. P. 1049–1053. https://doi.org/10.1364/AO.52.001049.

Authors and CV

Ali Qader Baki received the B.Sc. degree in Laser and Optoelectronics Engineering from the Laser and Optoelectronics Engineering Department, University of Technology, Baghdad, Iraq in 2010 and the M.Sc. degree in Optoelectronics Engineering from the Laser and Optoelectronics Engineering Department, University of Technology, Baghdad, Iraq in 2017. He is currently a Ph.D. student at the Institute of Laser for Postgraduate Studies, University of Baghdad, and a member in Quantum Optics and Electronics Group.
E-mail: ali.qader1101a@ilps.uobaghdad.edu.iq,
https://orcid.org/0009-0007-9057-7135

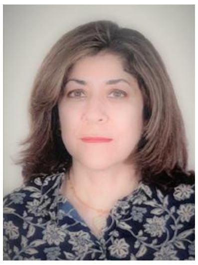

Shelan Khasro Tawfeeq received the B.Sc. degree from the College of Engineering, University of Baghdad, Baghdad, Iraq in 1990 and the M.Sc. and Ph.D. degrees from the Institute of Laser for Postgraduate Studies, University of Baghdad in 2001 and 2006, respectively. She is currently an Assistant Professor at the Institute of Laser for Postgraduate Studies, University of Baghdad and the Head of the Quantum Optics and Electronics Group. She is involved in research on applications of quantum optics in communication.
https://orcid.org/0000-0003-0908-9518

Authors' contributions

Baki A.Q.: methodology, numerical design and results investigation, data curation, writing – original draft.
Tawfeeq S.K.: conceptualization, methodology, review & editing, project administration.

Чисельне дослідження одношарових та міжшарових ґраткових поляризаторів на основі метаповерхневих структур для систем розподілу квантових ключів

A.Q. Baki, S.K. Tawfeeq

Анотація. Поляризація є важливою властивістю світла, яка характеризує напрямок коливань електричного поля. Модуляція поляризації відіграє важливу роль у розподілі квантових ключів з використанням поляризаційного кодування. Поляризацію використовують для кодування фотонів у системах розподілу квантових ключів. У цій роботі за допомогою чисельних методів, використовуючи програмне забезпечення COMSOL Multiphysics, було спроєктовано та досліджено поляризатори видимого діапазону з оптимальними розмірами на основі хвилеводів з резонансною ґраткою. Було розроблено дві структури: поляризатор з ґраткою на основі одношарової метаповерхні та поляризатор з ґраткою на основі міжшарової метаповерхні. Обидві структури продемонстрували високі значення коефіцієнта екстинкції, що дорівнювали $\sim 1.8 \cdot 10^3$ і $\sim 8.68 \cdot 10^4$, а також значення ширини смуги пропускання у 45 та 55 нм відповідно для поляризаторів на основі одношарової та міжшарової метаповерхонь.

Ключові слова: квантова криптографія, резонансна ґратка, субхвильова ґратка, метаповерхні, поляризатор з дротяною ґраткою.